Bioelectrochemistry 77 (2010) 94–99

Contents lists available at ScienceDirect

Bioelectrochemistry

journal homepage: www.elsevier.com/locate/bioelechem

Carbon nanotubes based electrochemical biosensor for detection of formaldehyde released from a cancer cell line treated with formaldehyde-releasing anticancer prodrugs

Lilach Bareket [a], Ada Rephaeli [b], Gili Berkovitch [b], Abraham Nudelman [c], Judith Rishpon [a,*]

[a] Department of Molecular Microbiology and Biotechnology, Tel-Aviv University, Ramat Aviv, 69978, Israel
[b] Felsenstein Medical Research Center, Sackler Faculty of Medicine, Tel-Aviv University, Beilinson Campus, Petach Tikva, 49100, Israel
[c] Department of Chemistry, Bar Ilan University, Ramat Gan, 52900, Israel

ARTICLE INFO

Article history:
Received 31 March 2009
Received in revised form 24 June 2009
Accepted 30 June 2009
Available online 8 July 2009

Keywords:
Formaldehyde
Prodrugs
Glioblastoma
Butyric acid
Carbon nanotubes
Screen printed electrodes

ABSTRACT

This paper reports the development of an electrochemical biosensor for the detection of formaldehyde in aqueous solution, based on the coupling of the enzyme formaldehyde dehydrogenase and a carbon nanotubes (CNT)-modified screen-printed electrode (SPE). We monitored the amperometric response to formaldehyde released from U251 human glioblastoma cells situated in the biosensor chamber in response to treatment with various anticancer prodrugs of formaldehyde and butyric acid. The current response was higher for prodrugs that release two molecules of formaldehyde (AN-193) than for prodrugs that release only one molecule of formaldehyde (AN-1, AN-7). Homologous prodrugs that release one (AN-88) or two (AN-191) molecules of acetaldehyde, showed no signal. The sensor is rapid, sensitive, selective, inexpensive and disposable, as well as simple to manufacture and operate.

1. Introduction

1.1. Formaldehyde detection

Standard analytical methods for the detection of formaldehyde, including HPLC [1], chromatography [2], or fluorimetry [3], require toxic reagents or solvents and suffer from a number of interferences requiring time for apparatus setup and thus are impractical for real-time measurements. Electrochemical biosensors are considered a good alternative for formaldehyde detection because they provide real-time measurements, high sensitivity, and selectivity [4–7]. Several electrochemical biosensors based on alcohol oxidase [6,8] or formaldehyde dehydrogenase (FDH) [4,5,7] have been developed for formaldehyde determination. Alcohol oxidase catalyzes the intracellular oxidization of formaldehyde using O_2 as the electron acceptor to generate formic acid and hydrogen peroxide, whereas FDH-catalyzed oxidation reactions use NAD^+ as the electron acceptor, yielding formic acid and NADH. The main advantage of using NAD-dependent dehydrogenase-based biosensors is that O_2 does not interfere in formaldehyde detection because it does not participate in the reaction [9]. The main drawback of such systems is the inefficient oxidation of the reduced co-factor NADH. The electrocatalytic oxidation of NADH requires high overpotential, where unwanted interference reactions and electrode fouling can occur [10–12].

1.2. NADH detection

Achieving the optimal overpotential for the electrochemical oxidation of NADH depends on the solvent type and pH [11]. Such high overpotential, approximately 0.6 V at pH 7, enables the oxidation of other electro-active species as well, resulting in anodic signal interference during the course of the analysis. As the measured signal does not represent the actual NADH oxidation, the sensor is less specific [13]. Moreover, fouling of the electrode surface resulting from radical intermediate accumulation and adsorption physically blocks the excess of new, unoxidized material from reaching the electrode surface. The main product of the reaction, NAD^+, creates dimers that adsorb to and block the electrode surface. The fouling effect results in the loss of electrochemical activity, whereas both effects reduce the stability and sensitivity of the system. In addition, such high overpotential leads to the formation of an enzymatically inactive form of NAD^+, meaning that no effective and reversible recycling of the coenzyme can occur. The efficient recycling of NAD^+ enables shifting the equilibrium of the enzymatic reaction toward the products, resulting in a lower detection limit and higher sensitivity [11,13–15].

The approaches used for solving these problems include chemical redox mediators [11,13–18] or enzymes [11,19,20] that catalyze electron transfer, thus enabling low-potential measurements and/or

* Corresponding author. Tel./fax: +972 3 6409366.
E-mail address: Judithri@tauex.tau.ac.il (J. Rishpon).

1567-5394/$ – see front matter © 2009 Elsevier B.V. All rights reserved.
doi:10.1016/j.bioelechem.2009.06.016

protection on the electrode surface from fouling. New materials for electrode manufacture that will enable efficient NADH oxidation are constantly being sought [21,22], among them carbon nanotubes [23].

1.3. Carbon nanotubes

Carbon nanotubes (CNT) can be described as graphite sheets rolled up into nanoscale tubes (single-wall carbon nanotubes (SWCNTs), or with additional graphene tubes around the core of an SWCNT (multi-wall CNTs (MWCNTs) [24]. CNT have unique qualities and are characterized by mechanical strength and elasticity [25], electrical conductivity [26,27], and chemical stability [25,28]. In addition, their large length-to-diameter ratio provides a large surface-to-volume ratio, imparting an outstanding ability to mediate fast electron transfer kinetics for a wide range of electroactive species such as NADH or hydrogen peroxide [24,29]. This ability is expressed as an improvement in the reversibility of electrochemical reactions and an increase in the rate of electron transfer, leading to a reduction of working potential and an increase of current signal. Nugent et al., (2001) suggested two alternative explanations for these effects. One, that the porous structure created by the CNT bundles and their small dimension provide for better wettability of the electrode surface; and two, the unique electronic surface structure of the nanotube, due to its helicity, low dimensionality, and possible topological defects, contributes to a higher electron transfer rate [30]. During amperometric detection, CNT-modified glassy carbon electrodes reduce the overpotential (below that of standard carbon electrodes), which is necessary for NADH oxidation, as well as for preventing the electrode-fouling effect [23]. The improved performance of CNT-modified electrodes is attributed to the presence of oxygen-rich groups on the CNT surface and to the small dimensions, electronic structure, and high electrical conductivity of CNT [23,31,32].

1.4. Anticancer prodrugs of butyric acid that release formaldehyde

Differentiation-inducing agents modify cancer cell differentiation, whereby the cancer cells restrain their own growth and return to a normal growth rate [33,34]. Differentiation therapy provides an alternative, less toxic approach for cancer treatment to replace chemotherapy and γ-irradiation, which are aggressive, highly toxic, and often nonspecific. Butyric acid (BA) is a potent pleotropic anticancer agent [35] that specifically affects gene regulation by transcriptional and post transcriptional modifications, thereby inhibiting the proliferation of a wide variety of malignant cells [36,37]. Although potentially useful in differentiation therapy, BA in vivo displays low potency due to its rapid metabolism [38]. To overcome this problem, BA prodrugs have been synthesized that serve as molecular carriers for the efficient transport of BA to the target cells, significantly increasing the potency of the drug in situ [39].

The family of acyloxyalkyl ester prodrugs of the histone deacetylase (HDAC) inhibitory BA have the general formula $Me(CH_2)_2COOCH(R)OR^1$, where R = H, Me, Pr, *tert*-Bu; R^1 = OC-alkyl, OC–Ar and $P(O)(OEt)_2$ [40,41]. The prodrugs upon hydrolytic degradation by intracellular esterases release acids and aldehydes [42]. Two types of BA prodrugs have been characterized: Type I, which undergoes intracellular metabolism releasing two carboxylic acids and an aldehyde, and Type II, which releases two aldehydes and three carboxylic acids (Fig. 1).

Formaldehyde plays a dominant role in the proliferation inhibition and apoptosis of cancer cells [42]. An additional property of such prodrugs is their ability to affect drug-resistant cancer cells. Formaldehyde up-regulates p53 and p21 expression and is a critical anti-proliferative factor that induces differentiation and cell death [42]. As the compound does not inhibit HDAC and has no effect on histone acetylation, the specific effects of formaldehyde on cell viability and differentiation are presumably mediated by different mechanisms. Recently, formaldehyde-releasing prodrugs were shown to diminish the level of glutathione (GSH), most likely by forming S-formylglutathione adducts, resulting in a decrease of free GSH and increase of reactive oxygen species followed by signaling events leading to cancer cells death [43]. Therefore, one can deduce that the reduction of cellular GSH by formaldehyde-releasing prodrugs represents one major mechanism by which the prodrugs promote cell death. Formaldehyde-releasing prodrugs were shown to synergistically augment the anticancer activity of doxorubicin by a unique mechanism of covalent adduct formation. For this to occur, the doxorubicin must react with cellular formaldehyde to form an activated Schiff base which is then able to form an aminal (N–C–N) linkage to the exocyclic amino group of guanine residues. The mono-adducts form primarily at G of 5′-GCN-3′ sequences [44].

To facilitate research on other mechanisms of action and the synergistic effects of formaldehyde and BA, as well as the kinetics of other formaldehyde releasing prodrugs, the ability to quantify formaldehyde release from cells in culture and in biofluid after treatment with prodrugs is essential. In this work, we present a novel amperometric biosensor for formaldehyde detection in aqueous solution, based on a CNT-modified screen-printed electrode (SPE) and FDH. We used the human glioblastoma cell line U251, situated in the biosensor chamber, treated with various BA-releasing prodrugs as an experimental model to examine the efficacy of the prodrugs.

2. Materials and methods

2.1. Reagents

Multi-wall carbon nanotubes (MWCNTs) (15 ± 5 nm in diameter) were purchased from Nanolab Inc. USA, FDH (E.C. 1.2.1.4) from *Pseudomonase putida* (specific activity of 3–5 U/mg), NAD^+ from yeast, formaldehyde (HCHO) 37% wt solution in water, glycine and DMSO

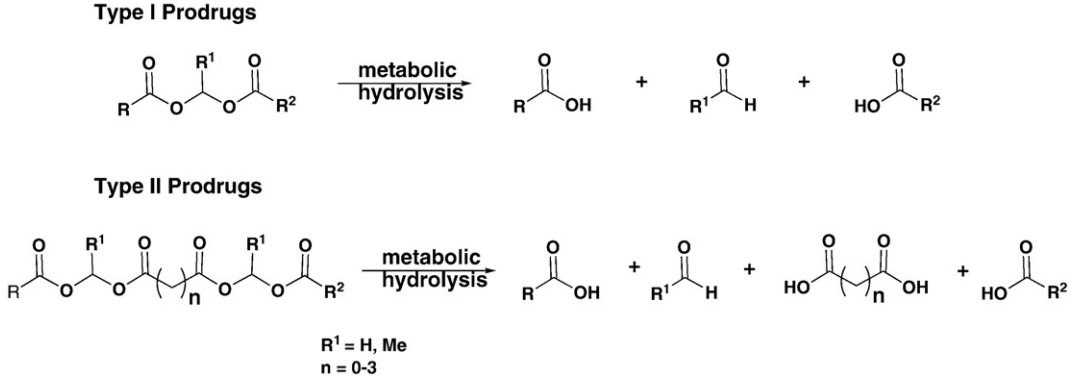

Fig. 1. Butyric acid derivatives type I (A) and type II (B) and their enzymatic cleavage products.

Table 1
The chemical structures of the prodrugs used in our work and their enzymatic hydrolysis products.

Prodrug	Structure	Hydrolysis products (no. equivalents)
Butyroyloxymethyl butyrate (AN-1)	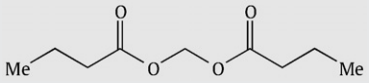	2 butyric acid 1 formaldehyde
Butyroyloxymethyl-diethyl phosphate (AN-7)	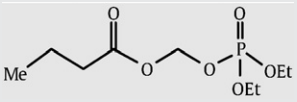	1 butyric acid 1 formaldehyde 1 phosphoric acid 2 ethanol
Butyroyloxydiethyl phosphate (AN- (88	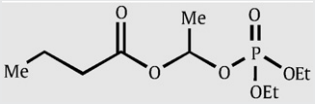	1 butyric acid 1 acetaldehyde 1 phosphoric acid 2 ethanol
Succinic acid dibutyryloxymethyl ester (AN-193)	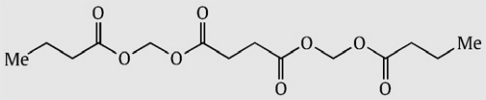	2 butyric acid 1 succinic acid 2 formaldehyde
Succinic acid bis-(1-butyryloxy-ethyl)ester (AN-191)	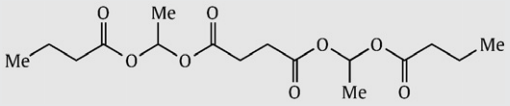	2 butyric acid 1 succinic acid 2 acetaldehyde

were purchased from Sigma. Before use, buffer solutions were prepared with analytical grade Na_2HPO_4, KCl, KH_2PO_4, K_2HPO_4, NaCl, NaOH purchased from Merck. All reagents and electrolyte solutions were prepared using double distilled water. The antibiotic mixture (penicillin 10,000 U/mL, streptomycin 10 mg/mL, nystatin 1250 U/mL), trypsin 0.25% and glutamine 29.2 mg/mL were purchased from Biological Industries. RPMI medium and FCS serum were purchased from GIBCO. Table 1 describes the butyric acid prodrugs and their metabolic hydrolysis products, which were synthesized as described [42].

2.2. Cell lines and cultures

Human glioblastoma cells, U251, were grown in RPMI medium containing 10% FCS serum, 1% glutamine and 1% antibiotic mixture at 37 °C in 95% air, 5% CO_2. The electrochemical measurements were performed in PBS using whole cells.

2.3. Screen printed electrodes modification

Screen printed electrodes (SPEs) were purchased from Gwent Electronic Materials, UK. The electrodes consisted of a carbon working electrode (3 mm diameter), a carbon auxiliary electrode, and an Ag/AgCl/0.1 M KCl reference electrode. A 0.6 cm diameter polystyrene cylinder was glued around the active area of the SPE creating a 300 μL micro-electrochemical cell, in which all the electrochemical measurements were performed. For preparing the SPE/CNT electrode, 3 μL of 40 μg/mL CNT suspension were dropped on the working electrode and dried for 30 min at 37 °C; the process was repeated three times to create a thicker CNT layer.

2.4. Electrochemical measurements setup

The CV50-W Bioanalytical system (BAS) computer controlled potentiostat was used. Formaldehyde dehydrogenase and NAD^+ were dissolved in the working solution. To obtain a cell suspension from a 50 mL growth bottle (containing ~2×10^6 cells), the growth medium in the bottle was discarded and the cell layer was rinsed twice with PBS. Then 1.5 mL of a 0.25% trypsin-EDTA solution was added to the cells and incubated for 4 min at 37 °C. The trypsinization was terminated by the addition of 5 mL PBS and centrifuging the cells for 4 min at 700 rpm. The pellet of the cells was suspended in 1.5 mL PBS and kept on ice during the experiment.

3. Results and discussion

3.1. Formaldehyde biosensor optimization

The formaldehyde biosensor involves the coupling of the formaldehyde dehydrogenase (FDH) enzyme with the coenzyme NAD^+ in a test solution and highly efficient NADH detection by a carbon nanotubes-modified screen-printed electrode (SPE/CNT). To assure the optimal analytical ability of the biosensor, we conducted a series of calibration experiments testing the following parameters: CNT

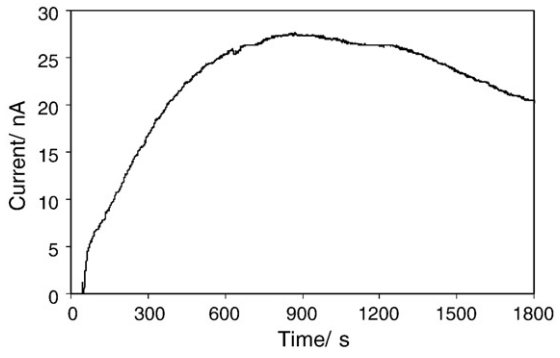

Fig. 2. Current signal measured in the SPE/CNT-based formaldehyde biosensor in response to the addition of 2 mM AN-193. Supporting electrolyte: PBS containing 0.5 mM NAD^+, 100 μg/ml FDH and U251 cells.

Table 2
Comparison between SPE and SPE/CNT based biosensors for the detection of formaldehyde released from U251 cells.

Electrode	Stationary current (nA)	STDEV
SPE	6.62	1.64
SPE/CNT	35.1	2.16

The stationary current from three separate experiments was measured 10 min after the exposure to 2 mM AN-193. Applied potential, 300 mV; supporting electrolyte: PBS containing 0.5 mM NAD^+, 100 μg/mL FDH and U251 cells.

optimal number of dried layers for NADH detection, NADH electro-oxidation potential, FDH concentration, NAD^+ concentration, and pH of the working buffer. The optimal parameters were three dried layers of 3 μL 40 μg/mL CNT solution dropped on the working electrode surface, 300 mV, 100 μg/mL FDH, 0.5 mM NAD^+ and pH 7.5 (data not shown). The calibration curve of the assay showed sensitivity over 0.1–1500 μM concentrations, with a linear range of 0.1–100 μM. Although the response was not linear beyond that, the biosensor remained sensitive to formaldehyde (data not shown). The electrochemical measurement was complete within 10 min.

3.2. Comparison between CNTs-modified and unmodified electrodes

A pretest checking the kinetics of formaldehyde release after prodrug treatment is presented in Fig. 2. Ninety-five percent of the peak current response was reached after 10 min, the time chosen for further analysis.

A comparison of the response of CNT-modified SPE and unmodified SPE 10 min after exposure to 2 mM AN-193 (three replicates) is presented in Table 2. The signal in response to formaldehyde on CNT/SPE was 5 times higher than that on the unmodified electrode.

3.3. Calibration

A calibration curve for formaldehyde detection in the presence of U251 cells is presented on Fig. 3. The current response to the direct addition of formaldehyde (data not shown)) was quicker and higher than the response to formaldehyde released after prodrug treatment (Fig. 2) 600 s vs. 900 s to reach stationary current. The time difference can be attributed to the time lapse between the minute the drug is released in the medium and enzymatic cleavage and diffusion of formaldehyde through the cell membrane back into the solution. The difference in signal intensity can be attributed to some formaldehyde remaining in the cells. Fig. 3 summarizes the calibration curve results from three replicates.

Table 3
Comparison between the current signals in response to different prodrugs.

Prodrug	Number of released formaldehyde molecules	Stationary current (nA)	STDEV
AN-1	1	22.61	5.51
AN-193	2	32.81	2.16
AN-191	0	0	0
AN-7	1	20.62	4.57
AN-88	0	0	0

The stationary average current from three separate experiments was measured 10 min after the exposure to 2 mM prodrug, by the SPE/CNT-based formaldehyde biosensor. The results presented in the table are after subtracting the background signals without cancer cells and without FDH. Applied potential, 300 mV; supporting electrolyte: PBS containing 0.5 mM NAD^+, 100 μg/mL FDH and U251 cells.

3.4. Comparison between formaldehyde released from different prodrugs

The signal induced by formaldehyde release after treatment with various prodrugs was tested. In addition, the background signals of the system were tested by adding the prodrug without FDH or without U251 cells, or by adding an equal volume of water instead of the prodrug. The results recorded after 10 min, subtracting the background signals, are summarized in Table 3. The current response was 1.5 times higher for prodrugs that release two molecules of formaldehyde (AN-193) than for prodrugs that release one molecule of formaldehyde (AN-1, AN-7). Prodrugs that release acetaldehyde (AN-88, AN-191) showed no signal.

Fig. 4 demonstrates the average stationary current response after 10 min to different concentrations of AN-193, which releases two molecules formaldehyde. A remarkable correlation ($y = 0.6583x - 1.786$, $R^2 = 0.9981$) was found between current signal and prodrug concentration. The reaction is linear up to 2 mM and it levels off thereafter, indicating the involvement of rate limiting step(s). Accumulation of extracellular formaldehyde is a function of the rates of AN-193 uptake into the cells, hydrolysis to formaldehyde by abundant cellular esterases, cellular metabolism of formaldehyde and the rate of formaldehyde efflux. Since the rates of AN-193 cellular breakdown and formaldehyde metabolism are unlikely to change substantially, and as a small molecule formaldehyde efflux by diffusion is rapid, the rate limiting step could be the uptake of AN-193.

3.5. The correlation between current signal and U251 cell concentration

The correlation between current signal and cell concentration was studied by adding 2 mM AN-193 to different dilutions of the cell containing the working solution (Fig. 5).

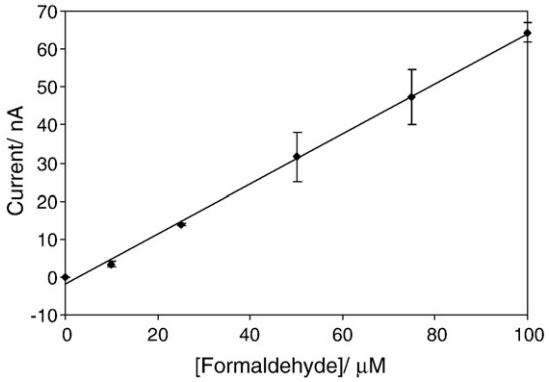

Fig. 3. Calibration curve for formaldehyde measured by the SPE/CNT-based biosensor. The error bars represent the standard deviation from three separate experiments. Applied potential, 300 mV; supporting electrolyte: PBS containing 0.5 mM NAD^+, 100 μg/mL FDH and U251 cells.

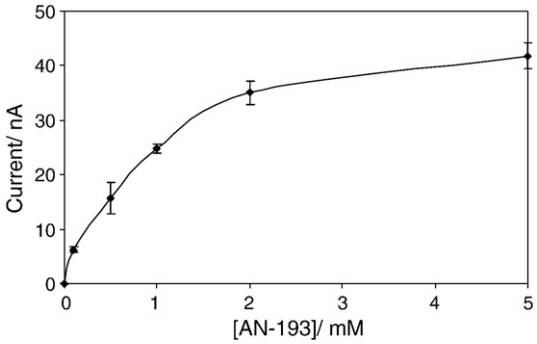

Fig. 4. Amperometric response to different concentrations of AN-193 (summarized results after 10 min). The error bars represent the standard deviation from three separate experiments. Applied potential, 300 mV; supporting electrolyte: PBS containing 0.5 mM NAD^+, 100 μg/mL FDH and U251 cells.

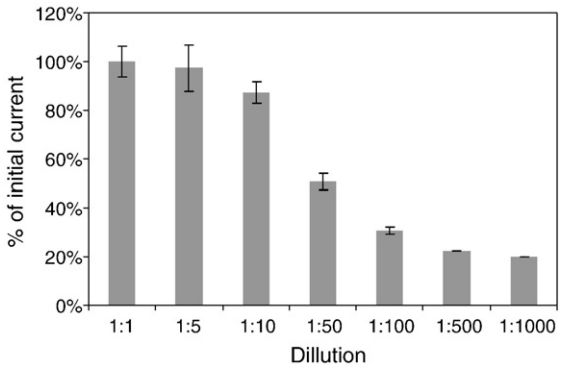

Fig. 5. Correlation between U251 brain cancer cells concentrations and induced formaldehyde release current signals presented as percentage from signal obtained for original solution (dilution 1:1). The error bars represent the standard deviation from three separate experiments. Applied potential, 300 mV; supporting electrolyte: PBS containing 0.5 mM NAD^+, 100 μg/mL FDH, 2 mM AN-193 and different dilutions of U251 original cell solution.

The finding of a distinct correlation between cell concentration and current signal confirmed that formaldehyde release resulted from an intracellular metabolic cleavage process.

4. Conclusions

We have presented a biosensor for the detection of formaldehyde based on coupling the selectivity of the enzyme FDH with the highly efficient NADH detection system using a CNT-modified SPE. The signal was five times higher on the SPE/CNT than on an unmodified SPE biosensor. The detection limit of the biosensor was 0.1 μM. The calibration curve of the assay covered five orders of magnitude (0.1–1500 μM concentrations), with a linear range of 0.1–100 μM (data not shown). The assay requires small amounts of sample and reagents (3–300 μL), and the electrochemical measurement is completed within 10 min.

The biosensor detected formaldehyde released from U251 human brain cancer cells in response formaldehyde-releasing anticancer prodrug treatment. The detection limit of direct formaldehyde addition in the presence of cells (10 μM) was higher than in clear buffer solution, probably due to the cells physically blocking formaldehyde access to the electrode surface, as well as to formaldehyde diffusing from the solution into the cells. The current response to formaldehyde released from prodrug-treated U251 cells was slower and lower than the response to direct formaldehyde addition. The time delay can be attributed to the process of prodrug diffusion into the cells, intracellular enzymatic cleavage, and the diffusion of formaldehyde back into the solution. The lower signal intensity can be attributed to part of the formaldehyde remaining in the cells.

Comparing the current signal measured following treatment with different prodrugs demonstrated, as expected, that the current was 1.5 times higher for prodrugs that release two molecules of formaldehyde (AN-193) than for those releasing only one molecule of formaldehyde (AN-1, AN-7), whereas prodrugs releasing acetaldehyde (AN-88, AN-191) showed no signal. Finally, the correlation between current signal and prodrug concentration and between cell concentration and current signal supports the notion that the formaldehyde release is a result of an intracellular hydrolysis of the prodrugs and diffusion of the released formaldehyde to the extracellular medium. The method of formaldehyde detection described herein is useful to study pharmacodynamics of formaldehyde-releasing prodrugs in cell cultures and bio-fluids.

References

[1] F. Sandner, W. Dott, J. Hollender, Sensitive indoor air monitoring of formaldehyde and other carbonyl compounds using the 2, 4-dinitrophenylhydrazine method, Int. J. Hyg. Environ. Health 203 (2001) 275–279.
[2] S. Kim, H.J. Kim, Comparison of standard methods and gas chromatography method in determination of formaldehyde emission from MDF bonded with formaldehyde-based resins, Bioresour. Technol. 96 (2005) 1457–1464.
[3] Y.Q. Zhen, S.E. Wang, W.X. Xiao, H.Y. Yuan, D. Xiao, A fluorescent dosimeter for formaldehyde determination using the Nash reagent in silica gel beads, Microchim. Acta 159 (2007) 305–310.
[4] Y. Herschkovitz, I. Eshkenazi, C.E. Campbell, J. Rishpon, An electrochemical biosensor for formaldehyde, J. Electroanal. Chem. 491 (2000) 182–187.
[5] R. Kataky, M.R. Bryce, L. Goldenberg, S. Hayes, A. Nowak, A biosensor for monitoring formaldehyde using a new lipophilic tetrathiafulvalene-tetracyanoquinodimethane salt and a polyurethane membrane, Talanta 56 (2002) 451–458.
[6] Y.I. Korpan, M.V. Gonchar, A.A. Sibirny, C. Martelet, A.V. El'skaya, T.D. Gibson, A.P. Soldatkin, Development of highly selective and stable potentiometric sensors for formaldehyde determination, Biosens. Bioelectron. 15 (2000) 77–83.
[7] F. Vianello, R. Boscolo-Chio, S. Signorini, A. Rigo, On-line detection of atmospheric formaldehyde by a conductometric biosensor, Biosens. Bioelectron. 22 (2007) 920–925.
[8] S.V. Dzyadevych, V.N. Arkhypova, Y.I. Korpan, A.V. El'skaya, A.P. Soldatkin, N. Jaffrezic-Renault, C. Martelet, Conductometric formaldehyde sensitive biosensor with specifically adapted analytical characteristics, Anal. Chim. Acta 445 (2001) 47–55.
[9] M.G. Zhang, C. Mullens, W. Gorski, Coimmobilization of dehydrogenases and their cofactors in electrochemical biosensors, Anal. Chem. 79 (2007) 2446–2450.
[10] J. Gebicki, A. Marcinek, J. Zielonka, Transient species in the stepwise interconversion of NADH and NAD(+), Acc. Chem. Res. 37 (2004) 379–386.
[11] I. Katakis, E. Dominguez, Catalytic electrooxidation of NADH for dehydrogenase amperometric biosensors, Mikrochim Acta. 126 (1997) 11–32.
[12] H.K. Chenault, G.M. Whitesides, Regeneration of nicotinamide cofactors for use in organic-synthesis, Appl. Biochem. Biotechnol. 14 (1987) 147–197.
[13] B. Grundig, G. Wittstock, U. Rudel, B. Strehlitz, Mediator-modified electrodes for electrocatalytic oxidation of NADH, J. Electroanal. Chem. 395 (1995) 143–157.
[14] B. Prieto-Simon, E. Fabregas, Comparative study of electron mediators used in the electrochemical oxidation of NADH, Biosens. Bioelectron. 19 (2004) 1131–1138.
[15] V.S. Vasantha, S.M. Chen, Synergistic effect of a catechin-immobilized poly(3, 4-ethylenedioxythiophene)-modified electrode on electrocatalysis of NADH in the presence of ascorbic acid and uric acid, Electrochim. Acta 52 (2006) 665–674.
[16] F. Pariente, F. Tobalina, G. Moreno, L. Hernandez, E. Lorenzo, H.D. Abruna, Mechanistic studies of the electrocatalytic oxidation of NADH and ascorbate at glassy carbon electrodes modified with electrodeposited films derived from 3, 4-dihydroxybenzaldehyde, Anal. Chem. 69 (1997) 4065–4075.
[17] N. Scherbak, A. Strid, L.A. Eriksson, Non-enzymatic oxidation of NADH by quinones, Chem. Phys. Lett. 414 (2005) 243–247.
[18] N.S. Lawrence, J. Wang, Chemical adsorption of phenothiazine dyes onto carbon nanotubes: toward the low potential detection of NADH, Electrochem. Commun. 8 (2006) 71–76.
[19] C. Ramirez-Molina, M. Boujtita, N. El Murr, New strategy for dehydrogenase amperometric biosensors using surfactant to enhance the sensitivity of diaphorase/ferrocene modified carbon paste electrodes for electrocatalytic oxidation of NADH, Electroanalysis 15 (2003) 1095–1100.
[20] T. Noguer, J.L. Marty, An amperometric bienzyme electrode for acetaldehyde detection, Enzyme Microb Technol. 17 (1995) 453–456.
[21] C.E. Campbell, J. Rishpon, NADH oxidation at the honey-comb like structure of active carbon: coupled to formaldehyde and sorbitol dehydrogenases, Electroanalysis 13 (2001) 17–20.
[22] M.J. Lobo, A.J. Miranda, P. Tunon, Amperometric biosensors based on NAD(P)-dependent dehydrogenase enzymes, Electroanalysis 9 (1997) 191–202.
[23] M. Musameh, J. Wang, A. Merkoci, Y.H. Lin, Low-potential stable NADH detection at carbon-nanotube-modified glassy carbon electrodes, Electrochem. Commun. 4 (2002) 743–746.
[24] M. Trojanowicz, Analytical applications of carbon nanotubes: a review, TrAc, Trends Anal. Chem. 25 (2006) 480–489.
[25] E. Katz, I. Willner, Biomolecule-functionalized carbon nanotubes: applications in nanobioelectronics, Chemphyschem 5 (2004) 1085–1104.
[26] J.J. Gooding, Nanostructuring electrodes with carbon nanotubes: a review on electrochemistry and applications for sensing, Electrochim. Acta 50 (2005) 3049–3060.
[27] K. Kaneto, M. Tsuruta, G. Sakai, W.Y. Cho, Y. Ando, Electrical conductivities of multi-wall carbon nano tubes, Synth. Met. 103 (1999) 2543–2546.
[28] K. Balasubramanian, M. Burghard, Biosensors based on carbon nanotubes, Anal Bioanal Chem. 385 (2006) 452–468.
[29] M.D. Rubianes, G.A. Rivas, Carbon nanotubes paste electrode, Electrochem. Commun. 5 (2003) 689–694.
[30] J.M. Nugent, K.S.V. Santhanam, A. Rubio, P.M. Ajayan, Fast electron transfer kinetics on multiwalled carbon nanotube microbundle electrodes, Nano Lett. 1 (2001) 87–91.
[31] G.A. Rivas, M.D. Rubianes, M.L. Pedano, N.F. Ferreyra, G.L. Luque, M.C. Rodriguez, S.A. Miscoria, Carbon nanotubes paste electrodes. A new alternative for the development of electrochemical sensors, Electroanalysis 19 (2007) 823–831.
[32] K.P. Gong, Y.M. Yan, M.N. Zhang, L. Su, S.X. Xiong, L.Q. Mao, Electrochemistry and electroanalytical applications of carbon nanotubes: a review, Anal. Sci. 21 (2005) 1383–1393.
[33] S. Sell, G.B. Pierce, Maturation arrest of stem-cell differentiation is a common pathway for the cellular-origin of teratocarcinomas and epithelial cancers, Lab. Invest. 70 (1994) 6–22.
[34] D.R. Bell, G. Van Zant, Stem cells, aging, and cancer: inevitabilities and outcomes, Oncogene 23 (2004) 7290–7296.

[35] V. Santini, A. Gozzini, B. Scappini, A. Grossi, P.R. Ferrini, Searching for the magic bullet against cancer: the butyrate saga, Leuk. Lymphoma 42 (2001) 275–289.
[36] J. Boren, W.N.P. Lee, S. Bassilian, J.J. Centelles, S. Lim, S. Ahmed, L.G. Boros, M. Cascante, The stable isotope-based dynamic metabolic profile of butyrate-induced HT29 cell differentiation, J. Biol. Chem. 278 (2003) 28395–28402.
[37] H. Newmark, M. Lipkin, Omega-3-fatty-acids and rectal epithelial-cell proliferation, Gastroenterology 107 (1994) 1892–1894.
[38] A.A. Miller, E. Kurschel, R. Osieka, C.G. Schmidt, Clinical-pharmacology of sodium-butyrate in patients with acute-leukemia, Eur. J. Cancer Clin. Oncol. 23 (1987) 1283–1287.
[39] Y. Zimra, A. Nudelman, R. Zhuk, E. Rabizadeh, M. Shaklai, A. Aviram, A. Rephaeli, Uptake of pivaloyloxymethyl butyrate into leukemic cells and its intracellular esterase-catalyzed hydrolysis, J. Cancer Res. Clin. Oncol. 126 (2000) 693–698.
[40] A. Nudelman, E. Gnizi, Y. Katz, R. Azulai, M. Cohen-Ohana, R. Zhuk, S.R. Sampson, L. Langzam, E. Fibach, E. Prus, V. Pugach, A. Rephaeli, Prodrugs of butyric acid. Novel derivatives possessing increased aqueous solubility and potential for treating cancer and blood diseases, Eur. J. Med. Chem. 36 (2001) 63–74.
[41] A. Rephaeli, E. Rabizadeh, A. Aviram, M. Shaklai, M. Ruse, A. Nudelman, Derivatives of butyric-acid as potential antineoplastic agents, Int. J. Cancer 49 (1991) 66–72.
[42] A. Nudelman, I. Levovich, S.M. Cutts, D.R. Phillips, A. Rephaeli, The role of intracellularly released formaldehyde and butyric acid in the anticancer activity of acyloxyalkyl esters, J. Med. Chem. 48 (2005) 1042–1054.
[43] I. Levovich, A. Nudelman, G. Berkovitch, L. Swift, S.M. Cutts, D.R. Phillips, A. Rephaeli, Formaldehyde-releasing prodrugs specifically affect cancer cells by depletion of intracellular glutathione and augmentation of reactive oxygen species, Cancer Chemother. Pharmacol. 62 (2008) 471–482.
[44] S.M Cutts, A Nudelman, A Rephaeli, D.R. Phillips, The power and potential of doxorubicin-DNA adducts, IUBMB Life. 57 (2005) 73–81.